Spectrochimica Acta Part B 122 (2016) 15–22

Contents lists available at ScienceDirect

Spectrochimica Acta Part B

journal homepage: www.elsevier.com/locate/sab

Investigating Early/Middle Bronze Age copper and bronze axes by micro X-ray fluorescence spectrometry and neutron imaging techniques☆

Elin Figueiredo [a,*], Marco A. Stanojev Pereira [b,c], Filipa Lopes [a,c,d], José G. Marques [c], Joana P. Santos [c], M. Fátima Araújo [c], Rui J.C. Silva [a], João C. Senna-Martinez [e]

[a] i3N/CENIMAT, Departamento de Ciências dos Materiais, Faculdade de Ciências e Tecnologia, Universidade NOVA de Lisboa, Quinta da Torre, 2829-516 Caparica, Portugal
[b] IPEN, Instituto de Pesquisas Energéticas e Nucleares, Centro do Reator de Pesquisas, Av. Prof. Lineu Prestes 2242, Cidade Universitária, 05508-000 São Paulo, Brazil
[c] C²TN, Centro de Ciências e Tecnologias Nucleares, Instituto Superior Técnico, Universidade de Lisboa, Estrada Nacional 10, km 139.7, 2695-066 Bobadela LRS, Portugal
[d] Departamento de Conservação e Restauro, Faculdade de Ciências e Tecnologia, Universidade Nova de Lisboa, Quinta da Torre, 2829-516 Caparica, Portugal
[e] UNIARQ, Centro de Arqueologia da Universidade de Lisboa, Faculdade de Letras, Universidade de Lisboa, Alameda da Universidade, 1600-214 Lisboa, Portugal

ARTICLE INFO

Article history:
Received 14 November 2015
10 May 2016
Accepted 17 May 2016
Available online 24 May 2016

Keywords:
Micro-XRF
Neutron tomography
Prehistoric axes
Metal composition
Internal structure

ABSTRACT

Micro X-ray fluorescence (micro-XRF) analysis and neutron imaging techniques, namely 2D radiography and 3D tomography, have been applied for the study of four metal axes from the Early/Middle Bronze Age in Western Iberia, a period characterized by a metallurgical change in the use of copper to bronze. Micro-XRF analysis has shown that one of the axes was produced in copper with some arsenic while the other three were produced in a copper-tin alloy (bronze) with variable tin contents and some arsenic and lead. Neutron radiography and tomography were applied to study internal heterogeneities of the axes in a non-invasive way since the specificities of neutron interaction with matter allow a suitable penetration of these relatively thick copper-based objects when compared to the use of a conventional X-ray radiography. Neutron imaging allowed the visualization of internal fissures and pores and the evaluation of their distribution, size and shape. Relevant information for the reconstruction of ancient manufacturing techniques was gathered, revealing that one ax was produced with the mold in an angle of ≈25°, probably to facilitate gas escape during metal pouring. Also, information regarding physical weaknesses of the axes was collected, providing relevant data for their conservation.

Novelty statement: The present paper combines the use of micro-XRF and neutron imaging techniques, namely (2D) radiography and (3D) tomography for the study of prehistoric metal axes. The XRF spectra allowed identifying major and minor elements present in the alloys, inferring on the absence of elements that could become radioactive for a long period of time after irradiation with neutrons. The specificities of neutron interaction with matter allowed a suitable penetration of these relatively thick copper-based objects when compared to the use of a conventional X-ray radiography.

The combination of these non-destructive techniques allowed the evaluation of the metal composition and the internal structure of the axes. Micro-XRF allowed the distinction among copper and bronze axes, and provided data about the composition of early bronzes for which data is scarce. The neutron imaging study allowed for the first time the visualization of internal heterogeneities in early bronze axes, namely pores and large voids, providing relevant information for the reconstruction of ancient manufacturing techniques and raising pertinent information regarding physical weaknesses of these types of objects.

1. Introduction

The study of archeological objects by diverse analytical and examination techniques brings information about the nature of the materials and the structure of the objects, contributing to the study of ancient manufacturing techniques and specific technological developments. Also, the possibility of evaluating any fragility of these cultural materials can serve to raise strategies for their future conservation.

One of the most emblematic type of archeological objects that were disseminated through Prehistoric cultures are axes. The first axes were made of stone, but with the advent of metallurgy, axes began to be made in the type of metal predominantly used during each chronological period. Thus, during the Copper Age axes began to be made of copper, and with the beginning of the Bronze Age axes began to be made of bronze. Bronze was the first intentionally man-made alloy, and was

☆ Selected paper from the Colloquium Spectroscopicum Internationale XXXIX (CSI 2015), Figueira da Foz, Portugal, 30 August–3 September 2015.

* Corresponding author.
E-mail address: emf12055@campus.fct.unl.pt (E. Figueiredo).

http://dx.doi.org/10.1016/j.sab.2016.05.002
0584-8547/

made by adding tin to copper in contents typically between 8 to 12 wt.%, although compositional differences can be found through time and space [1]. Comparing with copper, such bronze alloy has mechanical and color differences, such as a higher hardness and a golden hue, besides having a lower melting temperature that could provide some advantages in the production of cast objects.

In the present study a group of four flat axes attributed to the Early/Middle Bronze Age and found at different sites in the Portuguese territory were selected for an elemental and structural study. The axes are part of a larger collection at the Museu Nacional de Arqueologia (Lisbon, Portugal), and are from a chronological period characterized by the transition in the use of copper to the use of bronze in the Western Iberian territory. The four axes have their surfaces covered by corrosion, and some show the surfaces rather uneven. The axes have different sizes and slightly different shapes, and each one can be characterized by some particular feature: the ax 10853 is the smallest in length, but the thickest one (maximum thickness 1.5 cm); the ax 10240 is the thinnest (maximum thickness 0.6 cm) and lightest (208 g) and has some thin cracks, visible by the naked eye in the ax surface, that follows a path perpendicular to the main length; the ax 20138 is broken in two parts, being visible the presence of large pores in the fracture surfaces; the ax 32452 is the largest and heaviest (703 g), and shows the most uneven surface, with the presence of very rough areas (Table 1).

For elemental and structural studies of copper-based artifacts a large variety of analytical and examination techniques are nowadays available and used among the general scientific community. A technique capable of providing several advantages in the elemental characterization has been X-ray fluorescence spectrometry (XRF), due to its rather non-destructive character, providing multi-elemental identification in a wide range of concentrations. Also, the nowadays availability of commercial equipments in various formats and with diverse specificities, as macro-XRF, micro-XRF, portable and handheld XRF has contributed to its increasing use, including in non-laboratory contexts [2,3]. XRF elemental results have played an important role for the contextualization of objects into specific metallurgical contexts. In the Iberian Peninsula it has been shown that from Copper Age [4] until Early/Middle Bronze Age [5] coppers were used with arsenic in varying amounts (frequently 0–6 wt.% As) as a possible result from the use of As-rich copper ores. The first bronzes, which appeared during the Middle Bronze Age, could show a tendency to more irregular tin contents [6] than later bronzes, as those from the Late Bronze Age. The later ones would generally show absence of low tin bronzes, being tin frequently around 13 ± 2 wt.% [7]. Additionally, the presence of iron impurities in contents higher than 0.05 wt.% has been suggested to be related to more complex metallurgical extraction techniques, as those beginning in the Orientalizing/Iron Age [8,9].

Besides studies on the elemental characterization, one of the most fascinating aspects that can help in understanding ancient items is the ability to examine their internal structure. Transmission X-ray imaging techniques, as first radiography and lately tomography, has shown to be invaluable to the observation of internal features of various cultural artifacts without literally cutting into them and provoking physical damage. However, when it concerns metals, X-ray based techniques have a restricted contribution due to the limited penetration of X-rays among most metals, as those used in antiquity.

Table 2
Mass attenuation coefficients of Cu and Sn for thermal neutrons (25 meV) and X-rays (130 keV).

Element	Cu	Sn
Atomic mass	63.5	118.7
Density ρ (g/cm^3)	8.9	7.3
X-rays μ (cm^2/g)	0.28	0.84
Thermal neutrons μ (cm^2/g)	0.104	0.023

http://physics.nist.gov/PhysRefData/FFast/html/form.html and [17].

In order to overcome the limitation of X-rays, the use of neutron radiography has been emphasized back to half a century ago in some isolated works [10–11] where one of the most interesting advantages exposed was the possibility of examining organic objects lying behind thick metallic coatings: "X-rays are particularly useful for examining metals behind wood (…) but neutrons are better if the positions are reversed" [10].

The exploration of the differences between neutron imaging and the more conventional X-ray imaging techniques is still one of the topics most emphasized in the most recent published works dealing with the application of neutron radiography and tomography in cultural heritage [12–16]. Generally, these are: (1) high penetration of neutrons through metals; and (2) sensitivity of neutrons to hydrocarbons of all kinds. On the other hand, regular access to neutron infrastructures can be difficult, limiting the number of studies in the cultural heritage field. Also, since neutrons are able to activate materials by capture, there is the potential risk for radioactivity. Although copper and tin have relatively short half-lives (12.7 h and 27 h respectively), other elements that can be present in small concentrations in copper or bronze can stay activated for many days (e.g. Zn 244 days, Co 5.2 years, Ag 250 days) [14], preventing the artifacts to be handled shortly after the neutron analysis.

Like X-rays, neutrons penetrate objects and are attenuated by different elements to different extents. The remaining intensity I of an original intensity I_0 after penetration through a thickness x (cm) of material of density ρ (g/cm^3) and mass attenuation coefficient μ (cm^2/g) is:

$$I = I_0\, e^{-\mu\rho x}$$

While X-rays interact with electrons in the atomic shell, neutrons interact specifically with the nuclei of the atoms. As a result, attenuation of X-rays rises with increasing atomic number and density while with neutrons there is no direct relationship between atomic weight and transmission [14]. Regarding metals of ancient interest, the attenuation of neutrons in different elements follows the order Au > Ag > Fe > Cu > Pb > Sn (with neutrons being more attenuated in Au than Sn) while for X-rays is Pb > Au > Sn > Ag > Cu > Fe. Concerning the ancient Cu-Sn alloy (bronze), neutrons are more attenuated by Cu than by Sn, being the opposite to X-rays (Table 2).

In Fig. 1, the thickness of Cu and Sn materials for a remaining transmission of neutrons (soft neutrons, 25 meV) and X-rays (130 keV, a typical value for commercial X-ray scanners) behind the object is shown. It can be observed that for the same thickness of Cu or Sn materials the use

Table 1
Finding location and main physical characteristics of the studied axes.

Ax	Finding location	Mass	Size				
			Length	Width at blade	Width at top	Maximum thickness	Observations
10853	Gruta da Columbeira, Bombarral	360 g	9.2 cm	4.5 cm	2.0 cm	1.5 cm	Thickest
10240	Estremoz	208 g	9.6 cm	5.5 cm	2.5 cm	0.6 cm	Thinnest
20138	Campos de Grândola	471 g	6.4 + 5.4 cm	7.7 cm	3.4 cm	0.9 cm	Broken in 2 parts
32452	Minho	703 g	13.5 cm	8.0 cm	2.9 cm	1.3 cm	Largest

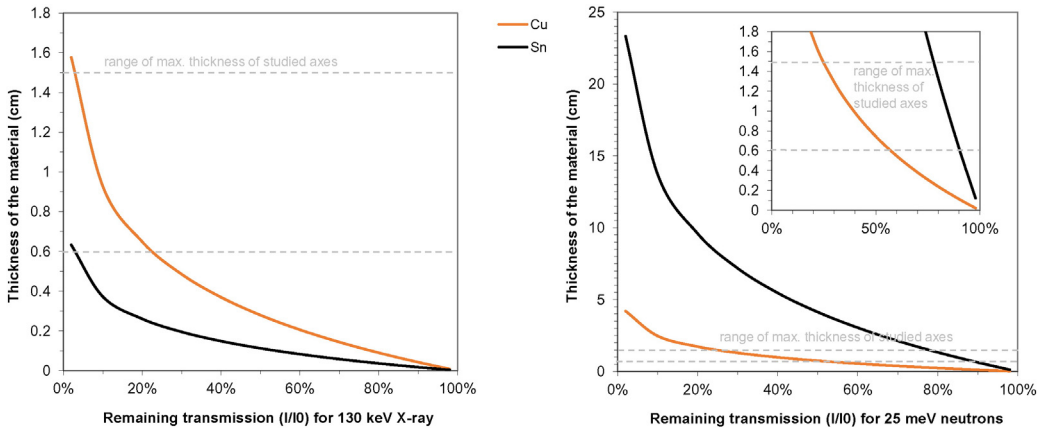

Fig. 1. Plots showing the remaining transmission behind copper and tin materials for X-rays (130 keV) and neutrons (25 meV). The range of the maximum thickness of the axes studied in this work is annotated.

of neutrons increases the transmission significantly comparing to X-rays. For thicknesses in the range of 0.6 to 1.5 cm (thicknesses of the axes) the remaining X-ray signal decreases from 23 to 2.5% for copper and is under 2.4% for tin, while for neutrons the remaining signal is comparatively higher, decreasing from 57 to 25% in copper and from 90 to 77% in tin. This clearly shows advantages of neutron imaging when copper or bronze objects with thicknesses in the range of the studied axes are to be examined.

In the present work an elemental and structural integrity study of the four axes from the Early/Middle Bronze Age is performed by micro X-ray fluorescence spectrometry and neutron imaging techniques. Results allow the evaluation of their composition and the characterization of internal features, such as material discontinuities, which can be relevant for understanding ancient manufacturing processes from this metallurgical transitional period.

2. Experimental

2.1. Micro-XRF

The determination of the alloy composition of the axes was performed by micro-energy dispersive X-ray fluorescence spectrometry (micro-XRF). In order to cause the minimum damage to the axes, the analyses were performed in small superficial areas (frequently $<5\ mm^2$) that were previously cleaned by removing the superficial corrosion patina.

The micro-XRF analyses were performed with an ArtTAX Pro spectrometer, with a low-power X-ray tube (30 W), a molybdenum anode and a polycapillary lens that generates a microspot of primary radiation ($\approx$70 μm in diameter) and a silicon drift detector with a resolution of 160 eV (Mn-Kα, FWHM) [18]. Axes were analyzed using 40 kV,

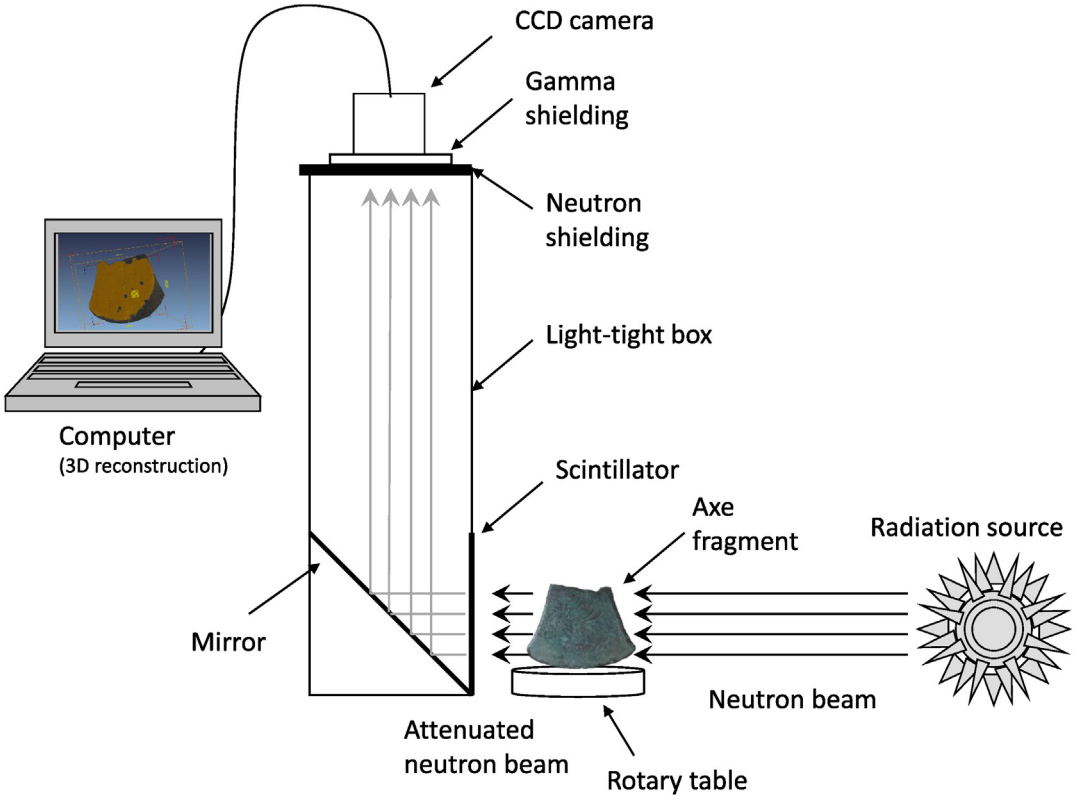

Fig. 2. Schematic representation of the setup for neutron imaging.

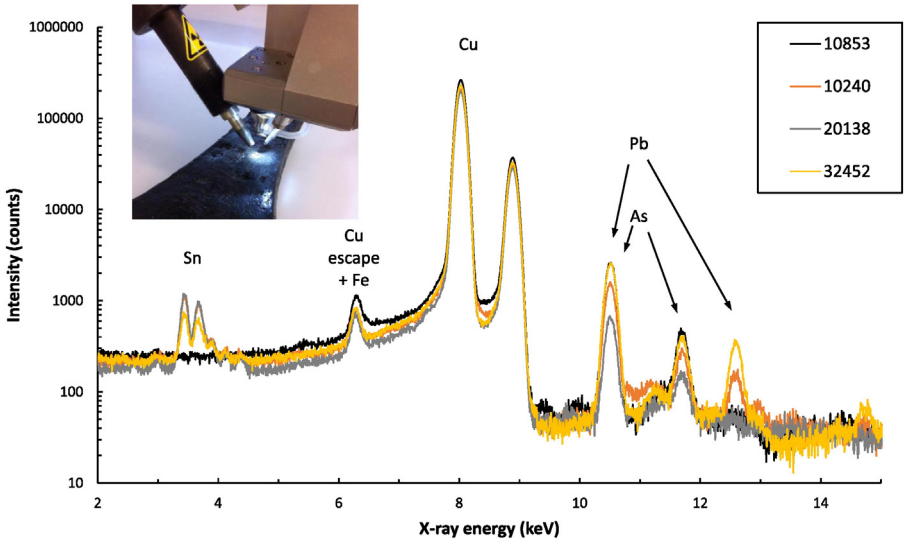

Fig. 3. One representative X-ray fluorescence spectrum acquired for each studied ax and an image of the analysis of ax 32452.

0.6 mA and 100 s of tube voltage, current intensity and live time respectively. Three analyses were made on different spots of the cleaned area of each ax to account for microheterogeneities, being considered the average value. The quantification analyses involved the WinAxil software and the use of reference materials (certified standards phosphor bronze 551 and 552 from British Chemical Standards and standard bronze 5 from Des Industries de la Fonderie). The accuracy of the method was established as having a relative error for major elements <5% and for minor elements <15%. Quantification limits were calculated as 0.04 wt.% for Cu, 0.5 wt.% for Sn, 0.1 wt.% for Pb and As, and 0.05 wt.% for Fe. More details on quantification procedures have been previously described and can be found in [7,19].

2.2. Neutron radiography and tomography

Neutron radiography (2D) and tomography (3D) were performed at the neutron tomography facility of the Portuguese pool-type 1 MW research reactor. This was the first time archeological metal artifacts were analyzed in this facility.

The neutron imaging facility has been installed at a horizontal access of the thermal column of the reactor, which is radial with respect to the reactor core. Samples are placed ≈50 cm away from the horizontal access in a rotary table, which enables objects to be rotated around a perpendicular ax in relation to the detector system, essential for tomography data acquisition. The flux of neutrons at sample irradiation position is 2.0×10^5 n·cm^{-2}·s^{-1}. Transmitted neutrons that pass through the samples are detected in a neutron scintillator placed behind the sample. The flux of the neutron beam at sample irradiation position is 2.0×10^5 n·cm^{-2}·s^{-1} and the diameter of the beam is about 5 cm. The neutron scintillator is coupled to a CCD video camera which in turn is coupled to a computer for image acquisition and processing. The spacial resolution of resulting image is 323 ± 11 μm. A scheme of the setup for neutron transmission radiation imaging is presented in Fig. 2. Further details have been described earlier, in [20].

Due to the relatively large size of the axes the radiographic study of each ax involved more than one individual radiographic image. To allow a complete image of the axes to be displayed three to eight individual radiographies had to be performed, and combined. The radiographic images were digitally treated, being presented with color inverted mode, and a contrast enhancement was performed to get a better visual perception of internal heterogeneities. Digital image-processing was made using Photoshop Elements software (http:/www.adobe.com/).

For each tomography the objects were rotated over 180°, in equal steps, during which projections were captured, processed and combined using Octopus software (http://www.inct.be/en/software/octopus) into 2D axial slices. The reconstruction of the 3D image of the whole volume was displayed using Fiji/Image J software with Volume Viewer plugin (http://www.fiji.sc/Fiji) [21].

3. Results and discussion

3.1. Elemental study by micro-XRF

The micro-XRF analysis made on the four axes showed that the smallest ax (10853) is made of copper, and the other three are made of Cu-Sn alloy (bronze) (Fig. 3). Other elements detected in small amounts were lead and arsenic, which have half-lives of only a few seconds to a few hours. The quantitative results show that all axes have small amounts of As (≈0.5–2.3 wt.%) and two bronze axes (10240 and 32452) do also show small amounts of Pb (≈0.5–1.4 wt.%) (Table 3).

The copper ax, with 2.3 wt.% As, can be understood in the context of a continuing use of coppers with varying arsenic contents from Copper Age until Early/Middle Bronze Age in Iberian Peninsula. On the other hand, the bronzes can be understood in the context of a new alloy that began to be used by the Middle Bronze Age, and can thus be interpreted as part of the first bronze axes from Western Iberian Peninsula.

Table 3
Results of micro-XRF analysis to the axes (results normalized; average of three analysis ± standard deviation; n.d. = not detected).

Ax	Type of metal	Composition (wt.%)				
		Cu	Sn	Pb	As	Fe
10853	Copper	97.6 ± 0.2	n.d.	n.d.	2.32 ± 0.14	<0.05
10240	Bronze	89.4 ± 0.1	8.87 ± 0.06	0.56 ± 0.14	1.19 ± 0.03	<0.05
20138	Bronze	90.7 ± 0.4	8.77 ± 0.35	n.d.	0.49 ± 0.02	<0.05
32452	Low tin bronze	92.1 ± 0.2	4.76 ± 0.13	1.36 ± 0.35	1.77 ± 0.15	<0.05

Within the bronzes, the Sn content is similar in two axes (10240 and 20138), with ≈9 wt.% Sn, which can be considered to be within the classical optimal tin quantity in a bronze alloy, 8–12 wt.% Sn, capable of providing a higher strength than pure copper but still allowing adequate thermo-mechanical processing. On the other hand, Sn is present in a smaller amount in the largest ax (32452), with ≈5 wt.% Sn, making this ax to be considered as a low tin bronze.

Previous analysis to ten bronze axes also attributed to the Early/Middle Bronze Age from the Portuguese territory [22] also identified one ax with a relatively lower tin content, with ≈6 wt.% Sn, which was explained as a result of the first attempts in bronze production. Possibly, during the transition from the use of copper to the full adoption of bronze, the manufacture of the alloy was not well established resulting in high variations in the tin content, with the presence of low tin bronzes. Also, since both copper and bronze would be in circulation, recycling processes involving both metals could result in the production of artifacts with decreasing tin contents. The low Pb and As contents found in the axes can be explained as ore impurity incorporations during smelting.

3.2. Examination of internal structures by neutron (2D) radiography

The radiographic images of the axes show some differences among them. The copper ax (10853) (Fig. 4) is the one that shows the most homogeneous structure, with no clear internal heterogeneities. Exception is a small hole at the top that is not an intrinsic feature of the ax, but is the result of a past sampling action performed in the 1950 or 60's in the context of the program *Studien zu den Anfängen der Metallurgie* undertaken by the Württembergisches Landesmuseum Laboratories, Stuttgart [23]. Such holes are also observed in the bronze axes.

Differing from the copper ax, the radiography of the bronze ax 10240 reveals stronger internal heterogeneities. The neutron attenuation differences, resulting in a lacy texture with diffuse outlines, can be a result of the concentrations of internal microporosities and/or a result of Cu/Sn distribution heterogeneities. It is known that bronzes with about 9 wt.% Sn can form two phases with different compositions, α-copper rich and δ phase with 32.6 wt.% Sn during regular cooling conditions as sand or stone mold casting. Such will favor a dendritic type microstructure, which can in turn result in the development of interdendritic shrinkage microporosities.

Additionally, in the radiography it is possible to observe the thin fissure that could also be observed at the upper part of the ax surface by the naked eye, indicating that the fissure is not superficial (i.e. has not developed only at the external corrosion layer) but is a deep fissure which has effectively developed into the bulk of the bronze ax. This information can provide important data for conservation strategies, as the ax is certainly more fragile at this region.

The radiographic image of the broken ax 20138 (Fig. 5) shows a lacy texture with diffuse outlines, similarly to the previous ax 10249, but does also show dispersed spherical or elongated-shaped heterogeneities of lower neutron attenuation. These are most likely internal pores, which can be a result of accumulated gas or air, trapped by the metal. A concentration of pores near the top of the ax and some dispersed pores in the lower half of the ax is visible. But the pores of larger size are located in the central region of the ax, where the fracture occurred. The break of this ax at this region can thus be associated to the presence of these large size pores (up to 1 cm in diameter) that must have significantly weakened the ax.

The radiography of the bronze ax 32452 shows a very peculiar and large size shaped heterogeneity at a central/top region of the ax. It can be described as a sphere-like shape with a tail-shaped part with a total length of ≈3 cm. Superficial observations on both sides of the ax did not show any particular feature at this region that could relate

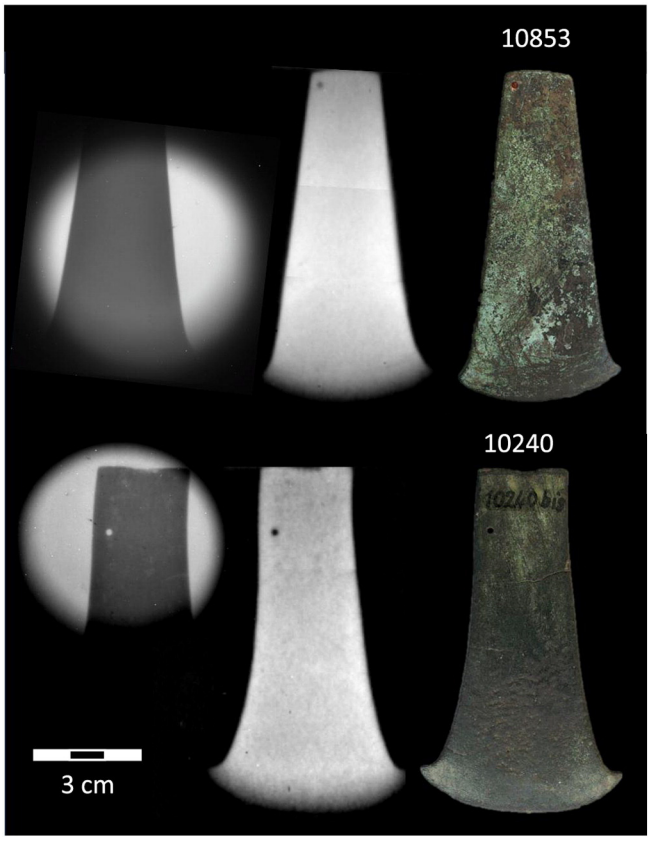

Fig. 4. Neutron radiography of the smallest size axes. At left one radiographic image as originally obtained (without digital treatment); at center radiographic image of entire ax by combining more than one individual radiograph and with inverted colors; at right the photograph of the original ax.

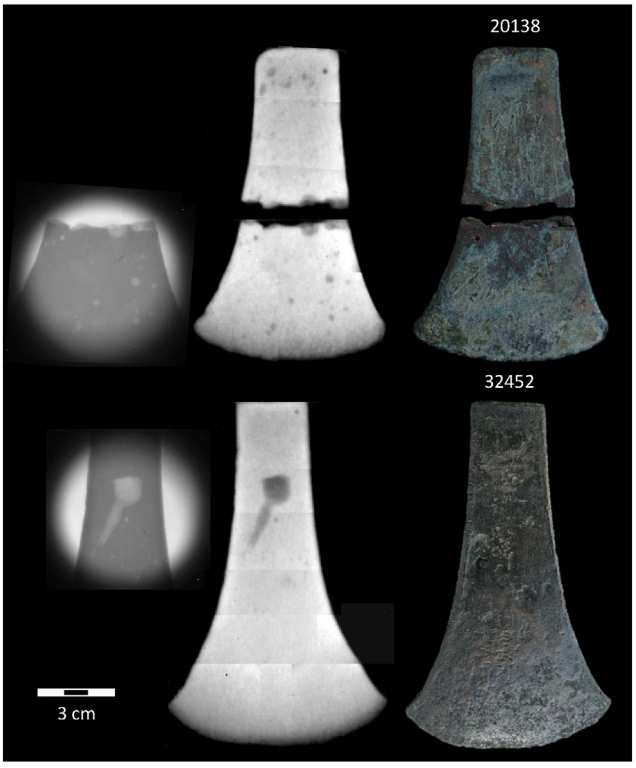

Fig. 5. Neutron radiography of the largest size axes. At left one radiographic image as originally obtained (without digital treatment); at center radiographic image of entire ax by combining more than one individual radiograph and with inverted colors; at right the photograph of the original ax.

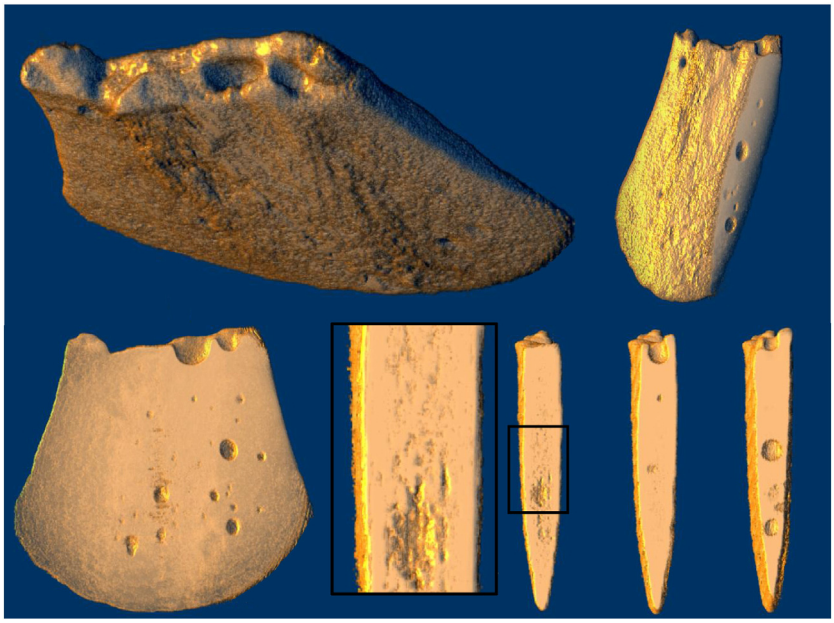

Fig. 6. Tomographic reconstruction of a volume of the lower half of the broken ax 20138 and virtual sections with incident virtual light to observe the distribution of internal macropores and microheterogeneities (detail at the center). (For scale information see Table 1 and Fig. 5).

directly to this internal heterogeneity. Only a small circular-shaped superficial heterogeneity of ≈0.5 cm ∅ located at one surface of the ax near the region of the end of the tail-shaped part could possibly be related. Given the lower neutron attenuation and the shape of this internal heterogeneity it can be suggested that it is a large gaseous void.

3.3. Examination of internal structures by neutron (3D) tomography

Based on the radiographic images, sections of volumes the axes 20138 and 32452 were selected for a detailed tomographic study.

The broken ax 20138 was subjected to a tomographic image in its lower half, in a volume that includes the fracture, in order to better determine the size and distribution of the pores, and thus contributes to the study of internal structural defects responsible for mechanical weaknesses.

The resulting tomography (Fig. 6) allowed the observation of various macropores distributed in the metal mainly towards the central regions. These pores were of variable sizes, being the largest ones in the range of 0.3–0.5 cm ∅. The exception is the ones present in the fractured area, which were of larger size, up to 1 cm. The presence of pores towards the central region of metal is a result of the advancing solidification fronts during casting, leading to a normal segregation of impurities, including gases, to the internal region that was the last part to solidify. In the present case it can be inferred that a relatively fast solidification process did not allow an effective escape of gas, resulting in macroporosities.

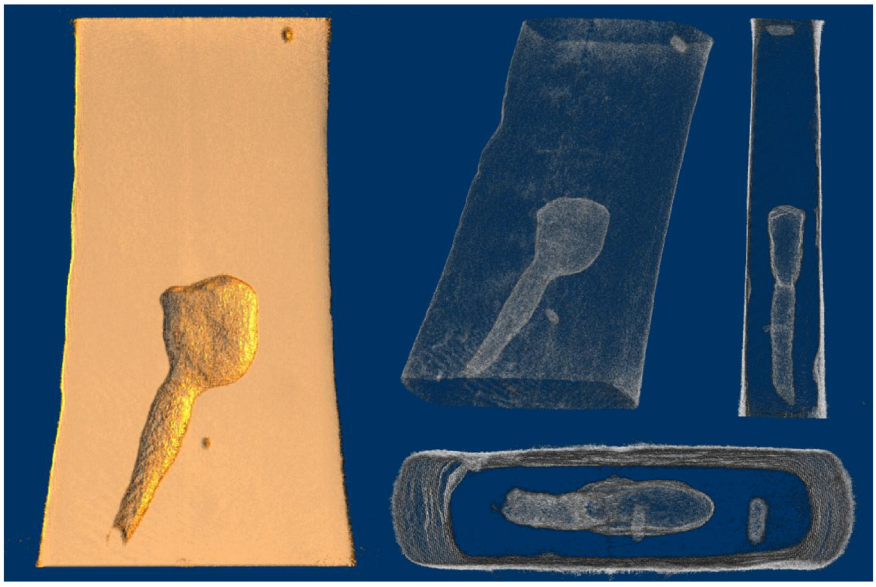

Fig. 7. Tomographic reconstruction of a volume of ax 32452. At left a virtual section with incident virtual light evidencing the large size internal void. At middle and right different views of the volume with the bronze material surfaces evidenced, to observe the shape and position of the internal large size void and two possible past sampled areas. (For scale information see Table 1 and Fig. 5).

Also, towards the central and lower parts of the tomographic volume small size heterogeneities, not totally resolved with the present neutron set-up resolution, which can be a concentration of microporosities, such as interdendritic micropores can be observed.

The ax 32452 was investigated by neutron tomography in the area where the large size void was detected. The tomographic reconstruction allowed a detailed examination of its position, size and shape (Fig. 7). It is observed that all the volume is positioned at a central region of the ax. Nevertheless, the end of the tail-shaped part makes a small turn in direction to the superficial heterogeneity identified during visual inspection, showing that some relationship could exist. Measurements of the void show that the semi-spherical part has a diameter of ≈1.4 cm and a max. thickness of 0.56 cm, while the tail-shaped part has a thickness in the range of 0.4–0.5 cm at its middle length.

The examination of tomography of the 32452 ax did also show the general absence for macropores distributed in the metal, contrasting with the previous examined broken ax 20138 which shows numerous pores distributed in the metal matrix at various regions. This can suggest that this large void represents the accumulation of gas/air from various regions of the metal. Only one small pore-like heterogeneity was found, placed in a central area, next to the large size void. But given its elongated shape, similar size and position/depth of penetration as the hole previously identified at the top of the ax as the result of a past sampling, this heterogeneity does also seem to be a past sampled area. Visual inspection of the surface of the ax does not show any clear evidence of these samples. However, the tomographic study makes clear their presence and shows that both were partially filled and covered, probably during some past restoration process.

The particular shape of the large void, composed by a sphere-like volume followed by a tail-shaped part in an angle of about 25° in relation to the vertical axis of the ax, suggests a moment of the escape of gas/air that became frozen in time due to a premature solidification of the metal. Based on its shape, it can be suggested that the mold was positioned at an angle of about 25° during the casting process, as shown in Fig. 8. Analysis to the shapes of several casting sprues from British Islands Bronze Age artifacts has shown that the pouring was frequently performed with the mold in an angle that could reach 30° [24]. This shows that possibly this was a casting procedure generally adopted for casting bronzes to facilitate the entrance of metal into the mold and simultaneously allowing the escape of air and gas. Nevertheless, this did not prevent that in some cases large amount of gases became entrapped, as in the present case. A poor gas escape could have had various reasons, such as a low pouring temperature or a not adequate preheating of the mold.

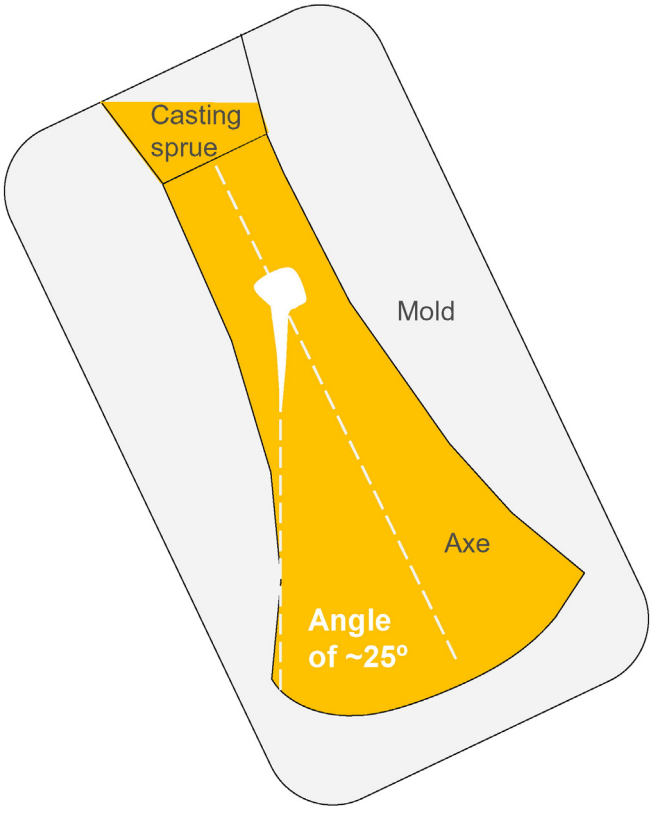

Fig. 8. Scheme of the probable mold position during metal pouring to cast the bronze ax 32452. The escape of gas/air is represented by the large size internal void (at white in the picture) that makes an angle of ≈25° with the main axis of the ax. (For scale information see Table 1 and Fig. 5).

4. Conclusions

The present study has shown the complementary use of elemental micro-XRF and neutron 2D and 3D imaging techniques for the study of relatively thick archaeologic metal artifacts, such as axes attributed to the Early/Middle Bronze Age.

The micro-XRF analysis is well suited for the investigation of small surface areas of the artifacts free of corrosion layers. The results have shown that while one ax was made of copper with arsenic, following the metallurgical tradition from Copper Age until Early/Middle Bronze Age, others were made of bronze, the new alloy that began to be introduced by the Middle Bronze Age in Western Iberia. In the bronze axes the Sn contents could vary, having two axes ≈9 wt.% Sn, within the classical optimal tin quantity in a bronze, while the other one had ≈5 wt.% Sn, being thus considered as a low tin bronze. Such low tin content is not commonly found during the later period (Late Bronze Age) when bronze was used in a generalized way, and can thus be explained as a result of the first attempts in bronze production or as a result of recycling.

The neutron radiographic and tomographic studies have been able to show, in a non-destructive way and for the first time in this type of metallic objects, the presence and dispersion of large pores among the internal structure of bronze axes. The copper ax was found to have a much more homogeneous internal structure. These pores were present mainly in the central zone of metal, which represents the last part of metal to solidify when casting into a closed mold. Also, a tendency for an accumulation of pores in the central to top regions was observed.

In the largest bronze ax a large void with a sphere-like and a tail-shaped part which allowed suggesting that the pouring of the metal was done with the mold in an angle of ≈25° was detected. The pouring with such an angle was most likely to allow gas escape. Nevertheless, as shown in the present work, this would not have been totally accomplished in many occasions. Additionally, in this ax, it was possible to detect past sampled areas which are nowadays invisible due to a posterior restoration treatment.

Finally, the micro-XRF analyses and neutron imaging investigation suggest that bronze axes from Iberian Middle Bronze Age can have fragile regions related to significant porosity, which can result into a subsequent fracture. Also, fragile zones can be present due to deep fissures, which should be taken into consideration for the conservation strategy of these items.

Acknowledgments

The authors would like to thank Dr. Luís Raposo, the former Director of the Museu Nacional de Arqueologia, and his team, for permission and collaboration for the study of the axes. This work was funded by FEDER funds through the COMPETE 2020 Program and National Funds through FCT -Portuguese Foundation for Science and Technology, under the project UID/CTM/50025/2013 to i3N/CENIMAT and the project UID/Multi/04349/2013 to C^2TN/IST. The grants SFRH/BPD/97360/2013 and SFRH/BD/85329/2012 by FCT to EF and FL are also acknowledged.

References

[1] C. Pare, Bronze and Bronze Age, in: C. Pare (Ed.), Metals Make the World Go Round: the Supply and Circulation of Metals in Bronze Age Europe, Oxbow Books, Oxford 2000, pp. 1–38.

[2] D. Šatović, V. Desnica, S. Fazinić, Use of portable X-ray fluorescence instrument for bulk alloy analysis on low corroded indoor bronzes, Spectrochim. Acta Part B 89 (2013) 7–13.

[3] V. Kantarelou, A.G. Karydas, D. Sokaras, L. Mahfouz, A. Qurdab, M. Al-Saadi, M. Giannoulaki, V. Argyropoulos, In situ scanning micro-XRF analyses of gilded bronze figurines at the National Museum of Damascus, J. Anal. At. Spectrom. 30 (2015) 1787–1798.

[4] R. Gauß, The development of metallurgy on the Iberian Peninsula. Technological and social patterns of a long-term innovation process, in: S. Burmeister, S. Hansen, M. Kunst, N. Muller-Scheeßel (Eds.), Metal Matters, Verlag Marie Leidorf GmbH, Rahden 2013, pp. 209–229.

[5] P. Valério, A.M.M. Soares, M.F. Araújo, R.J.C. Silva, L. Baptista, Middle Bronze Age arsenical copper alloys in southern Portugal, Archaeometry (2015), http://dx.doi.org/10.1111/arcm.12212.

[6] S. Rovira, I. Montero-Ruiz, Iberia: technological development of prehistoric metallurgy, in: S. Burmeister, S. Hansen, M. Kunst, N. Muller-Scheeßel (Eds.), Metal Matters, Verlag Marie Leidorf GmbH, Rahden 2013, pp. 231–239.

[7] E. Figueiredo, P. Valério, M.F. Araújo, R.J.C. Silva, A. Monge Soares, Inclusions and metal composition of ancient copper-based artefacts: a diachronic view by micro-EDXRF and SEM-EDS, X-Ray Spectrom. 40 (2011) 325–332.

[8] E. Figueiredo, M.F. Araújo, R.J.C. Silva, R. Vilaça, Characterisation of a Proto-historic bronze collection by micro-EDXRF, Nucl. Instrum. Methods Phys. Res., Sect. B 296 (2013) 26–31.

[9] P. Valério, R.J.C. Silva, A.M.M. Soares, M.F. Araújo, A.P. Gonçalves, R.M. Soares, Combining X-ray based methods to study the protohistoric bronze technology in Western Iberia, Nucl. Instrum. Methods Phys. Res., Sect. B 358 (2015) 117–123.

[10] J.P. Barton, Radiology using neutrons, Stud. Conserv. 10 (1965) 351-141.

[11] T.J.M. Robertson, Neutron radiography as a non-destructive tool in archaeology, Non-Destr. Testing 8 (1975) 17–20 (Guildford, England).

[12] E.H. Lehmann, P. Vontobel, E. Deschard-Erb, M. Soares, Non-invasive studies of objects from cultural heritage, Nucl. Instrum. Methods Phys. Res., Sect. A 542 (2005) 68–75.

[13] F.C. de Beer, H. Botha, E. Ferg, R. Grundlingh, A. Smith, Archaeology benefits from neutron tomography investigations in South Africa, Nucl. Instrum. Methods Phys. Res., Sect. A 605 (2009) 165–170.

[14] R. Van Langh, E. Lehmann, S. Hartmann, A. Kaestner, F. Scholten, The study of bronze statuettes with the help of neutron-imaging techniques, Anal. Bioanal. Chem. 395 (2009) 1949–1959.

[15] F. Koleini, F. de Beer, M.H. Alex Schoeman, I. Pikirayi, S. Chirikur, G. Nothnagel, J.M. Radebe, Efficiency of neutron tomography in visualizing the internal structure of metal artefacts from Mapungubwe museum collection with the aim of conservation, J. Cult. Herit. 13 (2012) 246–253.

[16] K. Ryzewski, S. Herringer, H. Bilheux, L. Walker, B. Sheldon, S. Voisin, J.-C. Bilheux, V. Finocchiaro, Neutron imaging of archaeological bronzes at the Oak Ridge national laboratory, Phys. Procedia 43 (2013) 343–351.

[17] P. von der Hardt, H. Röttger (Eds.), Neutron Radiography Handbook — Nuclear Science and Technology, Springer, Netherlands, 1981.

[18] H. Bronk, S. Rohrs, A. Bjeoumikhov, N. Langhoff, J. Schmalz, R. Wedell, H.E. Gorny, A. Herold, U. Waldschlager, ArtTAX — a new mobile spectrometer for energy-dispersive micro X-ray fluorescence spectrometry on art and archaeological objects, Fresenius J. Anal. Chem. 371 (2001) 307–316.

[19] P. Valério, M.F. Araújo, R.J.C. Silva, Complementary use of X-ray methods to study ancient production remains and metals from Northern Portugal, X-Ray Spectrom. 43 (2014) 209–215.

[20] M.I. Prudêncio, M.A.S. Pereira, J.G. Marques, M.I. Dias, L. Esteves, C.I. Burbidge, M.J. Trindade, M.B. Albuquerque, Neutron tomography for the assessment of consolidant impregnation efficiency in Portuguese glazed tiles (XVII century), J. Archaeol. Sci. 39 (2012) 964–969.

[21] J. Schindelin, I. Arganda-Carreras, E. Frise, et al., Fiji: an open-source platform for biological-image analysis, Nat. Methods 9 (2012) (2012) 676–682.

[22] E. Figueiredo, F. Lopes, M.F. Araújo, R.J.C. Silva, J.C. Senna-Martinez, E. Luís, Os primeiros bronzes do território Português: uma primeira abordagem arqueometalúrgica a um conjunto de machados Bujões/Barcelos, Estud. Arqueológicos Oeiras 19 (2012) 71–78 (in portuguese).

[23] S. Junghans, E. Sangmeister, M. Schröder, Metallanalysen kupferzeitlicher und frühbronzezeitlicher Bondenfunde aus Europa, Studien zu den Anfängen der Metallurgie 1, Gerb. Mann Verlag, Berlin, 1960 (in German).

[24] H.H. Coghlan, Notes on the Prehistoric Metallurgy of Copper and Bronze in the Old World, Occasional Papers on Technology, University Press, Oxford, 1975.